◆ EXPERIMENTAL INVESTIGATION ◆

Effect of Curvature on Displacement Forces Acting on Aortic Endografts: A 3-Dimensional Computational Analysis

C. Alberto Figueroa, PhD[1]; Charles A. Taylor, PhD[1,2]; Victoria Yeh[1]; Allen J. Chiou[1]; and Christopher K. Zarins, MD[2]

Departments of [1]Bioengineering and [2]Surgery, Stanford University, Stanford, California, USA.

Purpose: To determine the effect of curvature on the magnitude and direction of displacement forces acting on aortic endografts in 3-dimensional (3D) computational models.

Method: A 3D computer model was constructed based on magnetic resonance angiography data from a patient with an infrarenal aortic aneurysm. Computational fluid dynamics tools were used to simulate realistic flow and pressure conditions of the patient. An aortic endograft was deployed in the model, and the displacement forces acting on the endograft were calculated and expressed in Newtons (N). Additional models were created to determine the effects of reducing endograft curvature, neck angulation, and iliac angulation on displacement forces.

Results: The aortic endograft had a curved configuration as a result of the patient's anatomy, with curvature in the anterolateral direction. Total displacement force acting on the endograft was 5.0 N, with 28% of the force in a downward (caudal) direction and 72% of the force in a sideways (anterolateral) direction. Elimination of endograft curvature (planar graft configuration) reduced total displacement force to 0.8 N, with the largest component of force (70%) acting in the sideways direction. Straightening the aortic neck in the curved endograft configuration reduced the total force acting on the endograft to 4.2 N, with a reduction of the sideways component to 55% of the total force. Straightening the iliac limbs of the endograft reduced the total force acting on the endograft to 2.1 N but increased the sideways component to 91% of the total force.

Conclusion: The largest component of the force acting on the aortic endograft is in the sideways direction, with respect to the blood flow, rather than in the downward (caudal) direction as is commonly assumed. Increased curvature of the aortic endograft increases the magnitude of the sideways displacement force. The degree of angulation of the proximal and distal ends of the endograft influence the magnitude and direction of displacement force. These factors may have a significant influence on the propensity of endografts to migrate in vivo.

J Endovasc Ther. 2009;16:284–294

Key words: displacement forces, aortic endografts, endograft migration, abdominal aortic aneurysm, angulation, curvature, computational fluid dynamics

◆ ◆

This study was supported by the National Institutes of Health/NHLBI grant 2R01 HL64327-05A1. In accordance with the NIH Public Access Policy, this article is available for open access at PubMed Central.

Presented at International Congress XXI Endovascular Interventions held in Scottsdale, Arizona, USA, on February 10-14, 2008.

The authors have no commercial, proprietary, or financial interest in any products or companies described in this article.

Address for correspondence and reprints: Dr. Christopher K. Zarins, Department of Surgery, Clark Center E350A, 318 Campus Drive West, Stanford, CA 94305-5431 USA. E-mail: *zarins@stanford.edu*

Pulsatile aortic blood flow and pressure exert time-varying loads on all intra-aortic devices.[1–3] Long-term durability of these devices requires continuous mechanical fixation of the vascular prosthesis to prevent displacement.[4–6] Failure of fixation can lead to device migration and adverse clinical events, such as secondary interventions, endoleaks, rupture and death.[7]

A number of factors hypothesized to affect device migration have been clinically investigated, including aortic neck diameter, length, and angulation; neck calcification and thrombus; neck enlargement; inadequate proximal and distal fixation length; and neck enlargement.[8–10] In-vitro[11] and in-vivo experimental studies,[12] as well as theoretical[13] and computational studies,[14–19] have been conducted to investigate the magnitude of the loads acting on endografts. These loads have been referred to as migration forces, displacement forces, or drag forces. While some of these studies have analyzed several factors affecting migration forces, such as device size, hypertensive state, and different geometrical configurations, in all cases the reported forces have been assumed to act primarily in the downward (caudal) direction of blood flow. Experimental studies exerted linear downward displacement force on devices and computational studies considered devices in a planar and therefore idealized configuration. However, in humans, aortoiliac geometry is usually curved, with anterior angulation of the aneurysmal aorta and posterior curvature of the iliac arteries in the pelvis. This results in significant centerline lumen curvature of the aortoiliac segment and significant post-implantation curvature of implanted aortic endografts. In cases of severe aneurysm and aortic neck angulation, this curvature may be quite pronounced and may become more accentuated over time due to endograft migration. In this study, we investigated the impact of curvature on the displacement forces experienced by aortic endografts using a 3-dimensional (3D) computational technique.

METHOD

A 3D computer model of an abdominal aortic aneurysm (AAA) was constructed using a deidentified patient phase-contrast magnetic resonance angiography (MRA) dataset. The computer model included data from the supraceliac aorta to the iliac arteries, including the celiac, superior mesenteric, and renal arteries (Fig. 1).[20] Using the computer model,

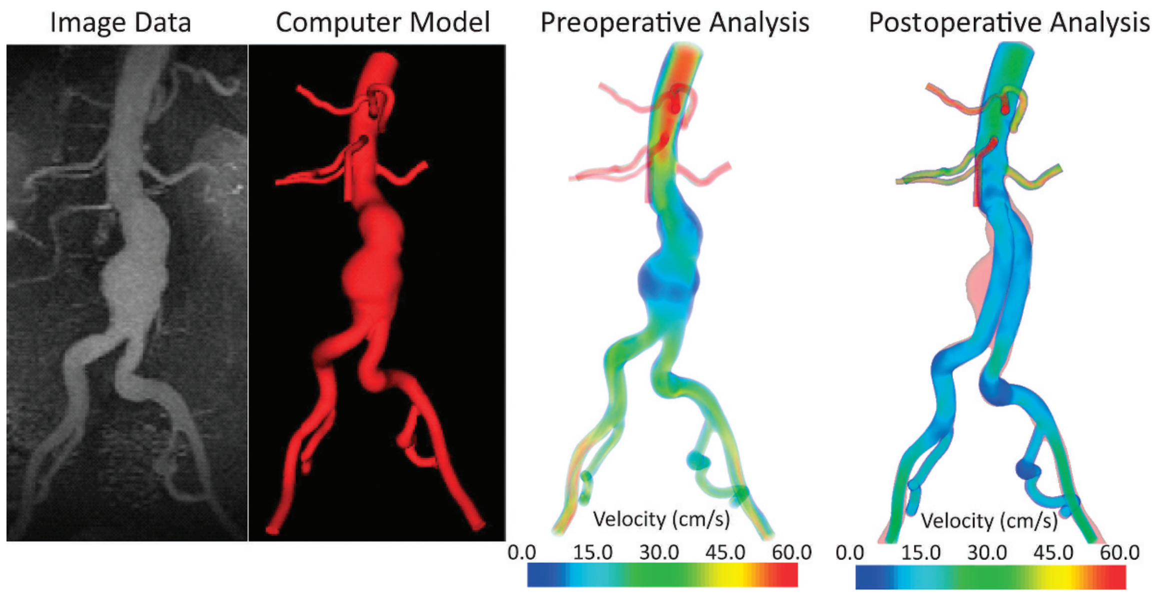

Figure 1 ◆ A 3D computer model was built based on the MRA dataset shown on the left. The preoperative CFD analysis is shown along with the post-endograft implantation CFD analysis.

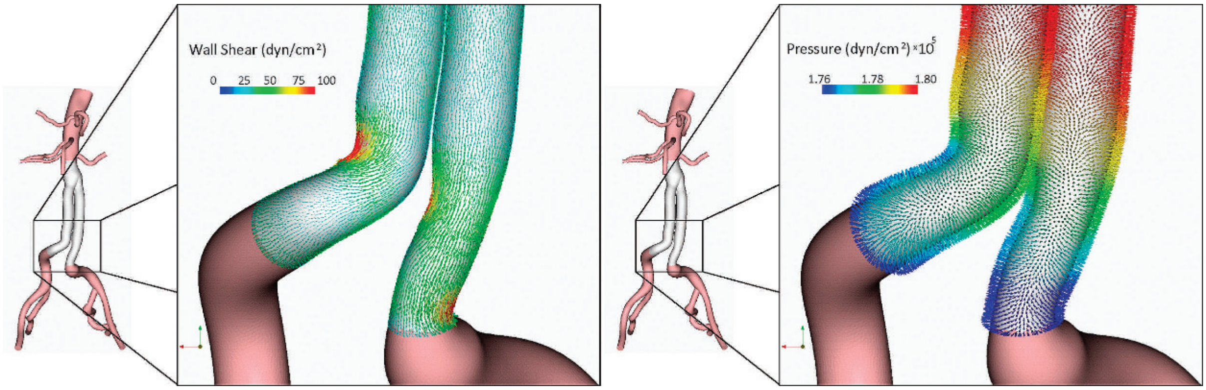

Figure 2 ◆ Wall shear (left) and pressure (right) stresses representing the actions of the blood on the endograft. These stresses are integrated over the surface of the endograft to calculate the total 3D force exerted by the pulsatile flow. Note that the pressure is several orders of magnitude larger than the shear stress. This fact, together with the main curvature of the graft, dictates the magnitude and orientation of the displacement force.

a computational fluid dynamics (CFD) analysis was performed to simulate blood flow and blood pressure.[21,22] In this analysis, additional patient-specific flow data [cine phase-contrast magnetic resonance imaging (PC-MRI)] at the supraceliac and infrarenal levels and pressure data (brachial pressure cuff measurements acquired immediately after the scan) were considered in order to model the baseline flow and pressure conditions in this patient as accurately as possible.[23] An aortic endograft was then virtually implanted in the aneurysm model and another CFD analysis was performed (Fig. 1). These flow and pressure baseline conditions remained unchanged in both the pre and post endograft simulations. The magnitude and direction of time-varying loads exerted by blood flow on the device were calculated by integrating the distribution of tractions (pressure and the shearing stresses) acting on the surface of the endograft (Fig. 2). The implanted endograft model was then modified to (a) eliminate endograft curvature, (b) straighten aortic neck angulation, and (c) straighten iliac angulation. For each endograft configuration, the magnitude and direction of displacement forces were calculated.

RESULTS

Preoperative Analysis

The results of the preoperative computational model are shown in Figure 3. Aortic inflow pressure matched the systolic (168 mmHg) and diastolic (92 mmHg) pressures measured in the patient. Individual branch flow waveforms varied depending on outflow boundary conditions of each vessel. The differences between the renal artery and iliac artery flow waveforms are shown with forward flow in the renal artery throughout the cardiac cycle and reversal of flow in the iliac artery during diastole, which represent normal physiological variations. The computed infrarenal aortic flow (1.4 L/min) matches the patient's measured aortic flow by PC-MRI at that location.

Post-Implantation Analysis: Curved Endograft

In this scenario, the dimensions of the endograft were chosen to reflect the sizes of the infrarenal aortic neck and the iliac arteries. The course of the endograft closely follows the preoperative aortic geometry and reflects the expected position of the endograft following deployment. The curvature of the endograft is described by the formula $C_1 = 1/R_1$, where R_1 is the radius that approximately fits a circle through the path of the graft; thus, the smaller the radius R_1 the larger the curvature of the endograft. The magnitude and vector of displacement force acting on the endograft in the AP (anteroposterior), lateral, and axial projections are shown by

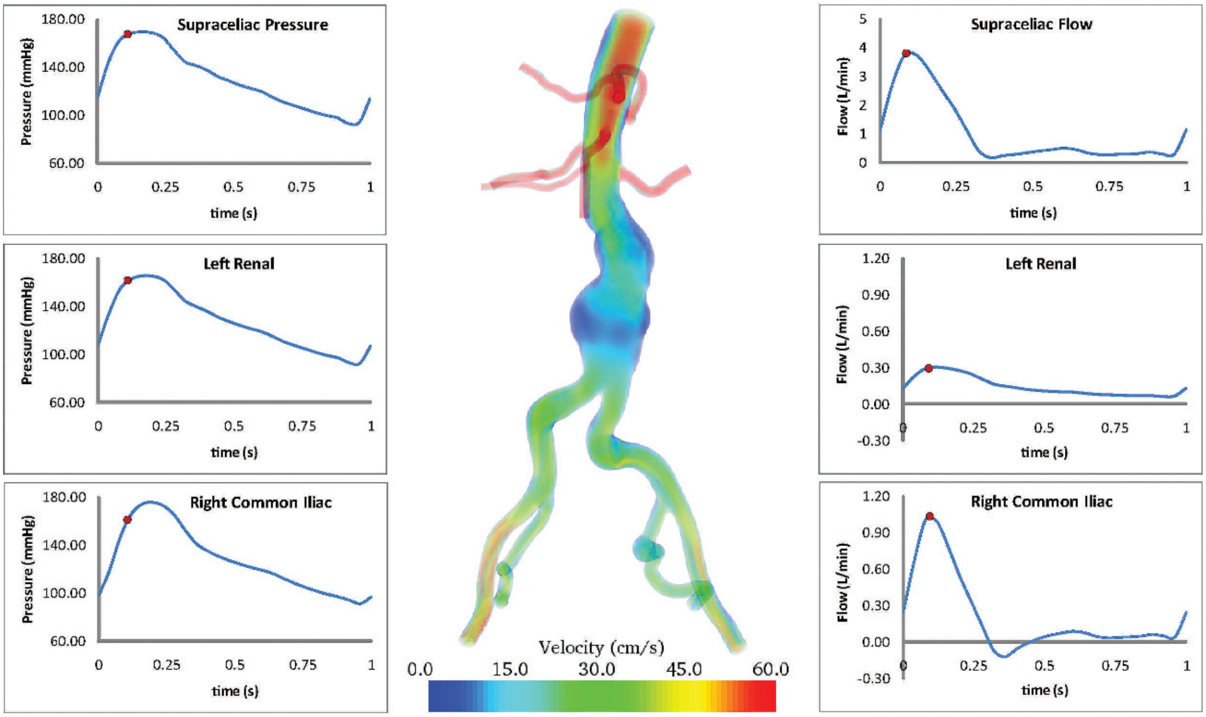

Figure 3 ◆ Preoperative CFD analysis of patient-specific computer model. Aortic inflow pressure and flow reflect the measured values in the patient at the time of PC-MRI measurements. Aortic, left renal artery, and right common iliac artery pressure and flow waveforms during 1 cardiac cycle are shown. Note: the time in the cardiac cycle shown in the velocity magnitude plot is indicated in the flow and pressure waves with a dot.

the size and direction of the arrows in Figure 4. The displacement force is primarily directed anteriorly and laterally and is largely in a sideways direction with respect to the axis of blood flow in the artery. The force vector appears to be largely determined by the curvature of the endograft.

Quantitative assessment of displacement forces acting on the endograft using CFD analysis is shown in Table 1. The 3D vector representing the temporal average of the total migration force reveals that the total displacement force acting on the endograft is 5.01 N; the largest components of force are in the anterior and lateral directions. The downward component of the force in the direction of blood flow, F_z, was relatively small compared to the sideways component, accounting for only 28% of the total force. Thus, 72% of the total displacement force was directed laterally or sideways with respect to the direction of blood flow.

Reduced Curvature (Planar) Endograft

The post-implantation computer model was altered to reduce endograft curvature by modifying the anatomy of the aorta in the region of the aneurysm to accommodate the endograft in an almost flat or planar configuration. The endograft dimensions and the aortic and branch flow and pressure conditions were unchanged. The curvature of the endograft was much reduced (Fig 5; $C_2 = 1/R_2$, $C_2 \ll C_1$). CFD analysis of the reduced curvature endograft revealed a significant (more than 5-fold) reduction in the total displacement force acting on the endograft to 0.8 N. The orientation of the displacement force vector was similar to that found in the curved endograft model (see Table 1), with 30% of the total force directed downward and 70% directed sideways. Thus, even in the reduced curvature model, the primary direction of displacement force was sideways with respect to the direction of blood flow.

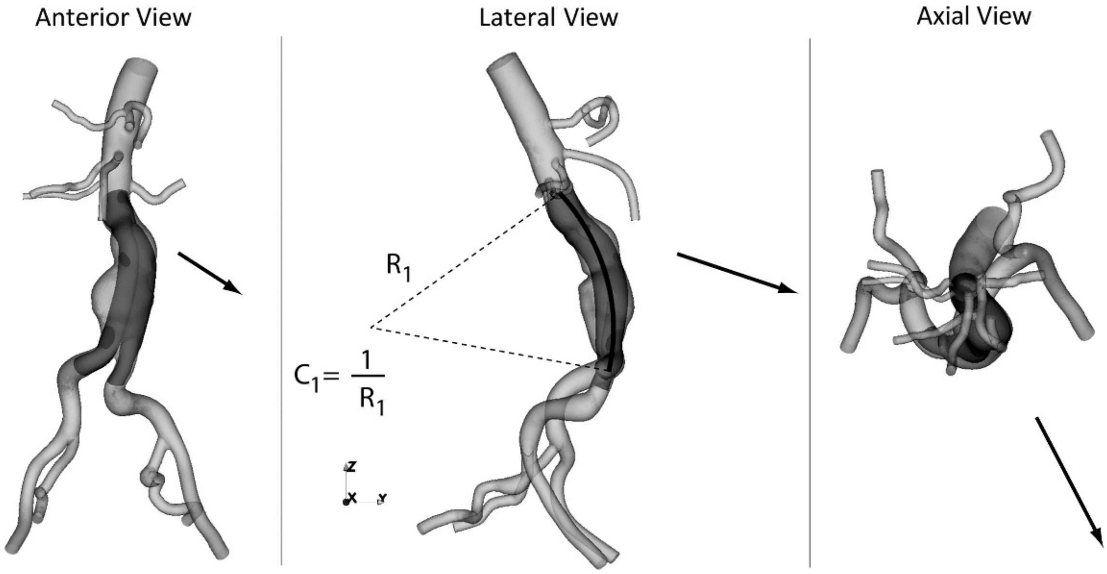

Figure 4 ◆ Anterior, lateral, and axial views of the aneurysm model with the aortic endograft in place. Note the anterolateral angulation of the endograft, which follows the curved anatomy of the aortoiliac segment. The vector of the displacement force is shown in each of the views.

Comparison of Curved to Planar Endograft

Comparing the pulsatile forces acting on the normally positioned curved endograft and the modified planar endograft, the flow and pressure conditions in both models were virtually identical (Fig. 6). As can be seen in the figure, the changes in endograft curvature did not alter the pressure field in the aorta significantly. However, there were marked changes in the total displacement force acting on the endograft. The temporal average total displacement force in the planar endograft was reduced by 5-fold to 0.8 N compared to the normally positioned curved endograft, which experienced a total force of 5 N. In both cases, the largest component of the force was F_y (i.e., anterior direction), which can be explained by the slight angulation of the neck of the abdominal aorta, directing the blood stream to impinge the endograft on the anterior face.

TABLE 1
Total and 3D Components of Displacement Force (F) for the Curved and Reduced Curvature Endografts

	Curved Endograft	Reduced Curvature Endograft
Fx (lateral), N	−2.22	−0.29
Fy (anterior), N	4.26	0.72
Fz (axial), N	−1.42	−0.24
Total force, N	5.01	0.81
% Downward	28.35	29.54

Aortic Neck and Iliac Angulation

The curved endograft model was modified to (a) reduce aortic neck angulation and (b) reduce iliac artery angulation. The magnitude and vector of total displacement force acting on the endograft are shown by the size and direction of the arrows in Figure 7. There were significant differences in both the magnitude and the direction of the displacement force for the 3 endograft configurations. The numerical values of the components of the force vector are shown in Table 2. The reduced neck angulation model showed a 17% reduction in displacement force compared to the normal curved model. The reduced iliac angulation model showed a 58% reduction in total displacement force compared to the normal curved model. The

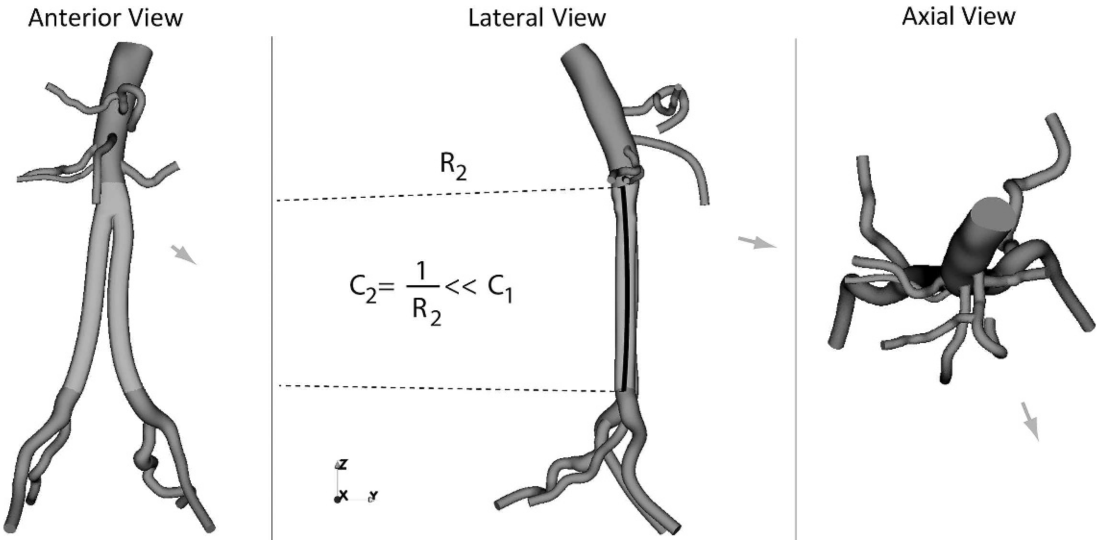

Figure 5 ◆ Anterior, lateral, and axial views of the reduced curvature endograft model in a planar configuration that removes the anteroposterior curvature of the endograft. The endograft dimensions are identical to the endograft shown in Figure 3. Note the reduction in magnitude of displacement force acting on the endograft as reflected by the size of the arrows. The direction of displacement force is similar to the curved configuration in Figure 3.

axial, or downward, displacement component was greatest for the straight aortic neck model (45% of the force of 4.2 N) and least for the reduced iliac angulation (9% of total force of 2.1 N). By comparison, the curved endograft model had a downward displacement component of 28%, with a total force of 5.01 N. In contrast, the sideways displacement force was greatest in the reduced iliac angulation model (91% of total of 2.1 N) and lowest in the reduced aortic neck angulation model (55% of total of 4.2 N).

DISCUSSION

Previous experimental and computational studies of aortic endograft fixation and migration have been based on the assumption that endograft displacement forces are directed downward, in the caudal direction of blood

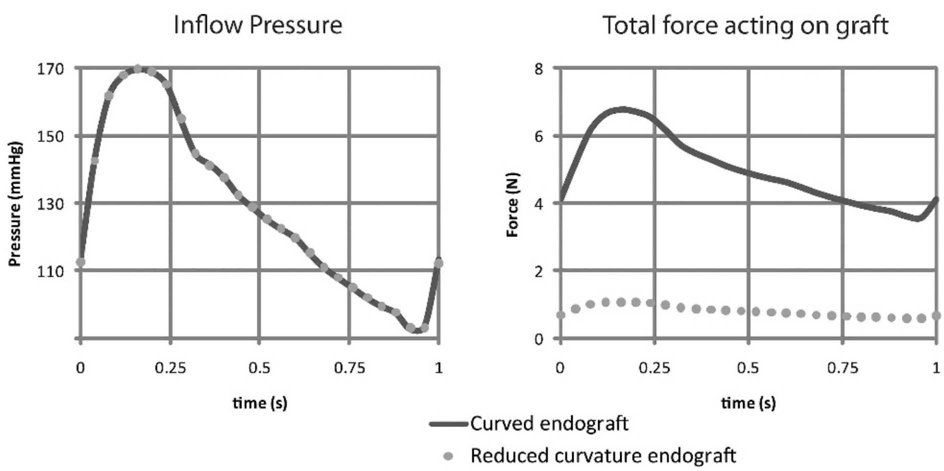

Figure 6 ◆ Comparison of normal curved endograft to reduced curvature (planar) endograft under the same pressure and flow conditions. The curved endograft has a 5-fold greater temporal average force (5.01 N versus 0.81 N) than the planar endograft model.

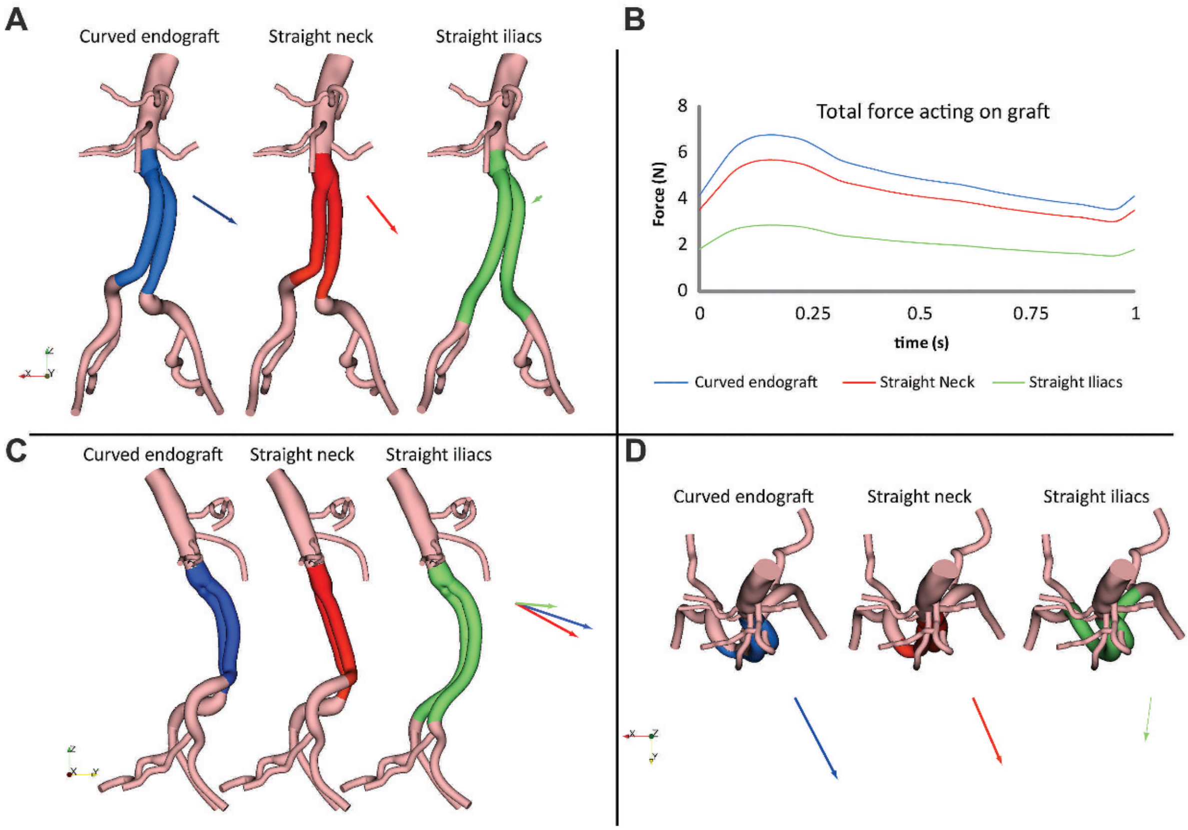

Figure 7 ◆ Effect of reducing aortic neck angulation and iliac angulation on total displacement force (**B**). The magnitude and direction of the displacement force vector are shown with arrows in the (**A**) anterior, (**C**) lateral, and (**D**) axial view.

flow. Current endografts are designed with a variety of fixation strategies to resist this downward displacement force. Nonetheless, all currently available endografts have experienced device migration. To our knowledge, no other 3D analysis of displacement forces acting on an aortic endograft has been done in a patient-specific aneurysm model that includes both the endograft geometry and the visceral branches (celiac, superior mesenteric, and renal arteries). Our findings in this anatomically realistic model show that the primary vector of displacement force acting on an aortic endograft is not downward in the direction of blood flow, but rather in a sideways direction or lateral to the axis of blood flow. Both the magnitude and vector of displacement force are greatly influenced by the curvature of the endograft. The greater the curvature of the endograft the greater the total displacement force acting on the endograft and the larger the sideways component of displacement. In addition to curvature of the endograft, angulation of the proximal aortic fixation zone and distal iliac fixation zone are important in determining endograft displacement force.

Almost all endografts have significant curvature due to the normal anatomy of the abdominal aorta, which is determined by the anterior angulation of the supraceliac aorta

TABLE 2
Total and 3D Components of Displacement Force (F) for the Curved Endograft, Straight Neck, and Straight Iliac Arteries Simulations

	Curved Endograft	Straight Neck	Straight Iliacs
Fx (lateral), N	−2.22	−1.48	0.28
Fy (anterior), N	4.26	3.43	2.09
Fz (axial), N	−1.42	−1.87	−0.19
Total force, N	5.01	4.18	2.12
% downward	28.35	44.76	8.97

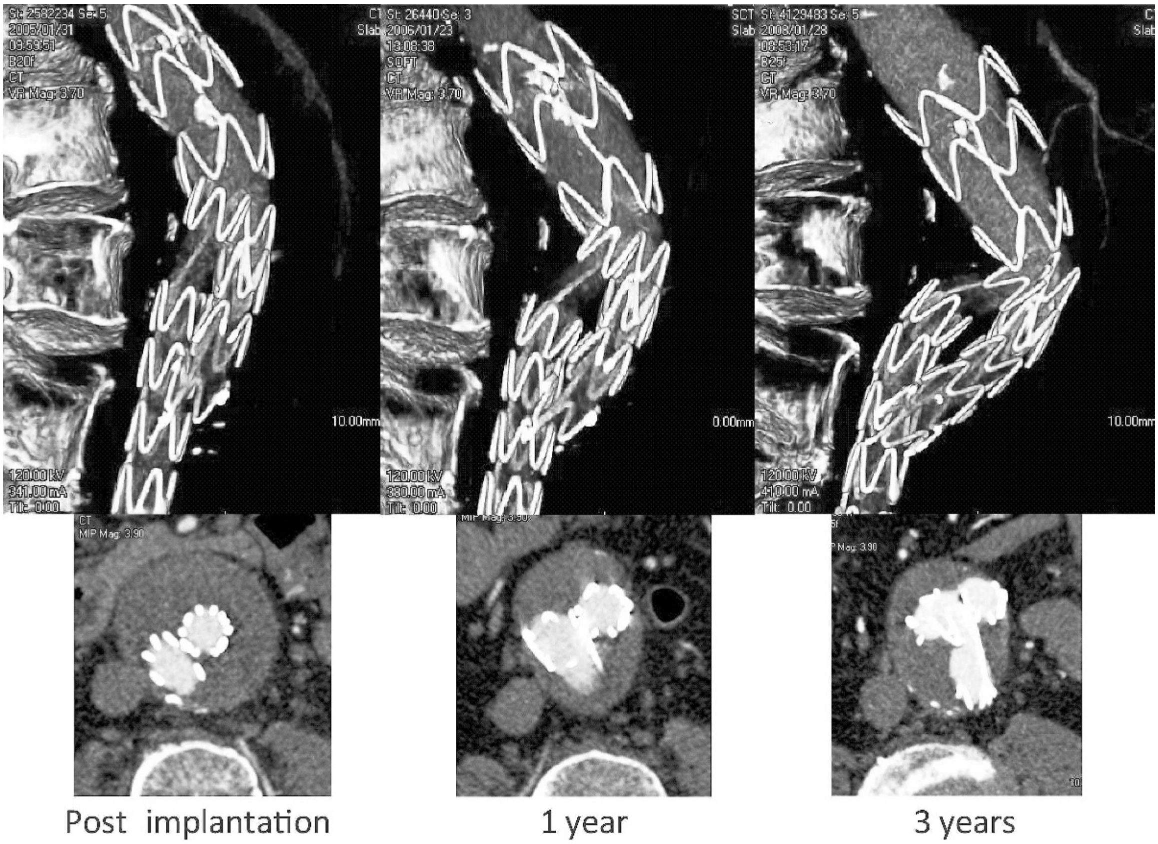

Figure 8 ◆ Lateral and cross-sectional CT images of an aortic endograft used to treat a patient with an abdominal aortic aneurysm. Note the anterior curvature of the endograft post implantation. There is anterior displacement of the aorta and endograft at 1 year with increased anterior displacement at 3 years. The movement is in the same direction of the sideways vector of displacement force demonstrated in the computational analysis. Note: these datasets correspond to a different patient than the one considered for the computational analysis.

and posterior curvature of the iliac arteries deep in the iliac fossa. This may not be apparent on the usual AP imaging of the aorta and is best appreciated on lateral or oblique image projections. Many aneurysms have great degrees of angulation and tortuosity, and the degree of endograft curvature is often much greater than the endograft modeled in this study. Greater degrees of endograft curvature will result in significantly larger forces applied to the endograft.

While clinical endograft migration is usually described as longitudinal or caudal migration,[3,24,25] image analysis often reveals significant lateral movement of the endograft, as depicted in Figure 8. The 5.5-cm aneurysm was treated with an endograft, and post-implantation computed tomography (CT) showed good position of the endograft with complete aneurysm exclusion and no endoleak. Lateral projection of the 3D CT image shows anterior curvature of the endograft, which is similar to the curved computational endograft model in this study. At 1 year, there was 1.6-cm anterior displacement of the endograft (Fig. 8); after 3 years, there was continued anterior endograft displacement, with 2.3 cm lateral movement of the endograft relative to the spine. The aneurysm remained unchanged in size, and there was no endoleak; however, there was significant movement of the endograft in the same direction as the sideways displacement force demonstrated in the computational model in this study.

A recent clinical study has shown that lateral movement of endografts within the aneurysm sac is an indicator of stent-graft instability. In a study of 60 high-risk patients treated with both suprarenal and infrarenal endografts, Rafii et al.[26] showed that lateral endograft movement within the aneurysm sac at 1 year was associated with an increased risk of late adverse events, including development of type I endoleaks, stent-graft migration, and the need for secondary procedures. Other reports of endograft migration have shown evidence of lateral endograft movement in published images,[27,28] which are consistent with the displacement force analysis findings in our study. The results presented here indicate that the total force experienced by AAA endografts in vivo greatly depends on the level of curvature to which these devices are exposed. This curvature is determined to some extent by the neck and iliac angulations, but it is also a function of the level of tortuosity of the aneurysm sac. Therefore, graft curvature in vivo might be an important predictor of migration, since we have demonstrated that geometries exposed to nearly identical levels of pressure experience very different migration forces. Our results show that the larger the curvature, the larger is the migration force for the same level of internal pressure.

Many patients treated with aortic endografts have severe degrees of aortic neck and iliac angulation and aneurysm tortuosity. These patients are likely to be at an increased risk of migration based on the migration forces acting on the endograft. In general, in tortuous geometries with important curvatures, the largest component of the migration force will be contained in the plane of the highest curvature. Currently available endografts have not been designed to deal with such degrees of tortuosity. Future endograft device design should take into consideration the orientation of the displacement force vector in order to ensure long-term stability of the device.

Limitations

Our simulations have been based on the assumption that the baseline supraceliac flow waveform and outflow boundary conditions for the untreated and stented AAA models remain unchanged. This is a reasonable first approximation for the resting conditions modeled since it is unlikely that repair of AAA will have much of an effect on the already low resistance of the infrarenal aortic segment under this low-flow state. As a result, since stent-graft implantation would be unlikely to alter the pressure drop across the infrarenal region (as the first graph of Figure 6 indicates), the effect on supraceliac flow waveform or the outflow boundary conditions would be expected to be minimal under resting conditions. In any event, further refinement of the inflow and outflow boundary conditions under resting conditions or the extension to higher flow states would require flow and pressure measurements before and after stent-graft implantation on a patient-specific basis.

In addition, we have assumed smooth lumen transitions of the endograft in both the neck and iliac regions. This is often not the case, particularly in cases of severe angulation, and this may affect the force analysis results presented here. We have also assumed that pressure in the aortic aneurysm sac after endograft deployment is zero. This is not the case in patients who have endoleaks after endovascular aneurysm repair.

Furthermore, these results have been obtained under the assumption that both the arterial and graft walls are rigid. However, both the aortic wall and endograft fabric may have varying degrees of movement. Future work, which includes the compliance of the vessel walls, is needed to evaluate how much changes in compliance might affect the forces experienced by endografts.[29]

Lastly, the analysis presented here provides just an estimate of the total force acting on an endograft. Actual endograft migration will depend not only on this force, but also on a number of other factors that are not considered in this analysis, such as the friction developed at the fixation points between the graft and the wall, fixation length, longitudinal columnar force, and the influence of penetrating hooks and barbs.

Conclusion

The primary orientation of the displacement force vector acting on an endograft implanted in an AAA is sideways rather than downward with respect to the direction of blood flow. The magnitude of the displacement force is greatly influenced by the curvature of the endograft; greater degrees of endograft curvature result in increased total and increased sideways-directed displacement force. Three-dimensional computational analysis may provide a powerful tool to evaluate the risk of endograft migration in vivo.

Acknowledgments: The authors gratefully acknowledge Andrea Les for the patient-specific image data, flow and pressure measurements, and computer model utilized for the preoperative analysis utilized in this work.

REFERENCES

1. Fogarty TJ, Arko FR, Zarins CK. Endograft technology: highlights of the past 10 years. *J Endovasc Ther*. 2004;11(Suppl II):II-192–II-199.
2. Zarins CK, Bloch DA, Crabtree T, et al. Stent graft migration after endovascular aneurysm repair: importance of proximal fixation. *J Vasc Surg*. 2003;38:1264–1272.
3. Zarins CK. Stent-graft migration: how do we know when we have it and what is its significance? [commentary] *J Endovasc Ther*. 2004;11:364–365.
4. Arko FR, Heikkinen MA, Lee ES, et al. Iliac fixation length and resistance to in-vivo stent graft displacement. *J Vasc Surg*. 2005;41:664–671.
5. Benharash P, Lee JT, Abilez OJ, et al. Iliac fixation inhibits migration of both suprarenal and infrarenal aortic endografts. *J Vasc Surg*. 2007;45:250–257.
6. Heikkinen MA, Alsac JM, Arko FR, et al. The importance of iliac fixation in prevention of stent graft migration. *J Vasc Surg*. 2006;43:1130–1137.
7. Sampram ES, Karafa MT, Mascha EJ, et al. Nature, frequency, and predictors of secondary procedures after endovascular repair of abdominal aortic aneurysm. *J Vasc Surg*. 2003;37:930–937.
8. Hobo R, Kievit J, Leurs LJ, et al. Influence of severe infrarenal aortic neck angulation on complications at the proximal neck following endovascular AAA repair: a EUROSTAR study. *J Endovasc Ther*. 2007;14:1–11.
9. Fulton JJ, Farber MA, Sanchez LA, et al. Effect of challenging neck anatomy on mid-term migration rates in AneuRx endografts. *J Vasc Surg*. 2006;44:932–937.
10. Zarins CK, AneuRx Clinical Investigators. The US AneuRx Clinical Trial: 6-year clinical update 2002. *J Vasc Surg*. 2003;37:904–908.
11. Resch T, Malina M, Lindblad B, et al. The impact of stent design on proximal stent-graft fixation in the abdominal aorta: an experimental study. *Eur J Vasc Endovasc Surg*. 2000;20:190–195.
12. Murphy EH, Johnson ED, Arko FR. Device-specific resistance to in vivo displacement of stent-grafts implanted with maximum iliac fixation. *J Endovasc Ther*. 2007;14:585–592.
13. Morris L, Delassus P, Walsh M, et al. A mathematical model to predict the in vivo pulsatile drag forces acting on bifurcated stent grafts used in endovascular treatment of abdominal aortic aneurysms (AAA). *J Biomech*. 2004;37:1087–1095.
14. Li Z, Kleinstreuer C, Farber M. Computational analysis of biomechanical contributors to possible endovascular graft failure. *Biomech Model Mechanobiol*. 2005;4:221–234.
15. Li Z, Kleinstreuer C. Analysis of biomechanical factors affecting stent-graft migration in an abdominal aortic aneurysm model. *J Biomech*. 2006;39:2264–2273.
16. Fung GS, Lam SK, Cheng SW, et al. On stent-graft models in thoracic aortic endovascular repair: a computational investigation of the hemodynamic factors. *Comput Biol Med*. 2008;38:484–489.
17. Morris L, Delassus P, Grace P, et al. Effects of flat, parabolic and realistic steady flow inlet profiles on idealised and realistic stent graft fits through abdominal aortic aneurysms (AAA). *Med Eng Phys*. 2006;28:19–26.
18. Howell BA, Kim T, Cheer A, et al. Computational fluid dynamics within bifurcated abdominal aortic stent-grafts. *J Endovasc Ther*. 2007;14:138–143.
19. Molony DS, Callanan A, Morris LG, et al. Geometrical enhancements for abdominal aortic stent-grafts. *J Endovasc Ther*. 2008;15:518–529.
20. Wilson NM, Wang KC, Dutton RW, et al. A software framework for creating patient specific geometric models from medical imaging data for simulation based medical planning of vascular surgery. In *Lecture Notes in Computer Science.* vol. 2208. Berlin: Springer; 2001:449–456.
21. Taylor CA, Hughes TJR, Zarins CK. Finite element modeling of blood flow in arteries. *Comput Meth Appl Mech Eng*. 1998;158:155–196.
22. Vignon-Clementel IE, Figueroa CA, Jansen KE, et al. Outflow boundary conditions for three-dimensional finite element modeling of blood flow and pressure in arteries. *Comput Meth Appl Mech Eng*. 2006;195:3776–3796.

23. Les AS, Figueroa CA, Draney Blomme MT, et al. Quantification of hemodynamics in abdominal aortic aneurysms during rest and exercise using magnetic resonance imaging and computational fluid dynamics. Presented at: *International Society for Magnetic Resonance in Medicine Conference*; Toronto, Canada; May 3–8, 2008.
24. Cao P, Verzini F, Zannetti S, et al. Device migration after endoluminal abdominal aortic aneurysm repair: analysis of 113 cases with a minimum follow-up period of 2 years. *J Vasc Surg*. 2002;35:229–235.
25. Parra JR, Ayerdi J, McLafferty R, et al. Conformational changes associated with proximal seal zone failure in abdominal aortic endografts. *J Vasc Surg*. 2003;37:106–111.
26. Rafii BY, Abilez OJ, Benharash P, et al. Lateral movement of endografts within the aneurysm sac is an indicator of stent-graft instability. *J Endovasc Ther*. 2008;15:335–343.
27. Krämer SC, Seifarth H, Pamler R, et al. Geometric changes in aortic endografts over a 2-year observation period. *J Endovasc Ther*. 2001;8:34–38.
28. Umscheid T, Stelter WJ. Time-related alterations of shape, position, and structure in self-expanding modular aortic stent-grafts. *J Endovasc Surg*. 1999;6:17–32.
29. Figueroa CA, Vignon-Clementel IE, Jansen KE, et al. A coupled momentum method for modeling blood flow in three-dimensional deformable arteries. *Comput Meth Appl Mech Eng*. 2006;195:5685–5706.